ARTICLE

doi:10.1038/nature13496

Patterning and post-patterning modes of evolutionary digit loss in mammals

Kimberly L. Cooper[1]†*, Karen E. Sears[2]*, Aysu Uygur[1]*, Jennifer Maier[2], Karl-Stephan Baczkowski[3], Margaret Brosnahan[4], Doug Antczak[4], Julian A. Skidmore[5] & Clifford J. Tabin[1]

A reduction in the number of digits has evolved many times in tetrapods, particularly in cursorial mammals that travel over deserts and plains, yet the underlying developmental mechanisms have remained elusive. Here we show that digit loss can occur both during early limb patterning and at later post-patterning stages of chondrogenesis. In the 'odd-toed' jerboa (*Dipus sagitta*) and horse and the 'even-toed' camel, extensive cell death sculpts the tissue around the remaining toes. In contrast, digit loss in the pig is orchestrated by earlier limb patterning mechanisms including downregulation of *Ptch1* expression but no increase in cell death. Together these data demonstrate remarkable plasticity in the mechanisms of vertebrate limb evolution and shed light on the complexity of morphological convergence, particularly within the artiodactyl lineage.

Tetrapod limbs evolved adaptations for running, swimming, flying and many other tasks, each reflected in functional modifications to their morphology. Digit reduction, a decrease in the number of digits from the basal pentadactyl (five-digit) morphology, arose repeatedly in tetrapod evolution[1]. There are two plausible developmental mechanisms by which this could take place. The first would be to specify fewer digit primordia during the time when developmental fates are patterned in the early limb bud. The second would be to initially organize the limb bud in a normal pentadactyl pattern but then fail to elaborate the full set of digits by resculpting the nascent limb through differential proliferation or cell death.

To date, the molecular developmental mechanism of evolutionary digit reduction has been explored in only one tetrapod group, the skinks of the genus *Hemiergis*. Distinct species of *Hemiergis* range in digit number from two to five[2,3], with evolutionary progression to fewer digits correlating with increasingly early termination of Sonic hedgehog (*Shh*) expression in the posterior limb bud[4]. *Shh* serves a dual purpose in limb development, both to pattern the digits and to expand the hand and foot plates to allow for the formation of a full complement of digits[5–7]. Experimental truncation of the developmental timing of *Shh* expression removes digits in the reverse order of their formation[7], consistent with a mechanism first suggested by Alberch and Gale[8], thus providing a convenient way to evolutionarily tweak digit number without disturbing the overall structure of the limb. However, this mechanism would not, in a simple manner, generate the symmetrical reduction of anterior (pre-axial) and posterior (post-axial) digits seen, for example, in the evolution of the horse lineage.

To investigate how digit reduction evolved in other adaptive contexts we examined the mode of digit loss in a bipedal three-toed rodent and in three ungulates: the single-toed horse, an odd-toed ungulate or perissodactyl, and the pig with four toes and the camel with two, each representing the even-toed ungulates or artiodactyls (Fig. 1a, b).

Mechanisms of digit loss in the three-toed jerboa

We first focused on the three-toed jerboa, *D. sagitta* (Fig. 1f). This species has several advantages in identifying meaningful alterations to ancestral developmental mechanisms. First, it has a close evolutionary relationship to the laboratory mouse and to a five-toed species of jerboa, *Allactaga elater*[9] (Fig. 1d). Moreover, digit loss in *D. sagitta* is limited to the hindlimb whereas forelimbs maintained five fully formed fingers[10,11]. This provides a unique opportunity to identify differences specific to morphological divergence of the hindlimb among a potential abundance of species-specific modifications shared in the development of both sets of paired appendages.

In the adult *D. sagitta*, the three central metatarsals are fused into a single element that trifurcates distally and articulates with each of the three digits[10]. However, in the neonate, alcian blue and alizarin red staining of the chondrogenic skeleton reveals that the three complete digits and their associated metatarsals are flanked by small, truncated cartilage remnants of the first and fifth metatarsals (Fig. 1c and Extended Data Fig. 1). This suggests that at least the proximal-most portion of each of the five digit rays is patterned early in development and that digits I and V are either not fully patterned distally or are truncated at a subsequent differentiation stage.

To gain a better sense of when the patterning and/or morphogenesis of the lateral digits begins to diverge in the three-toed jerboa hindlimb, we compared the contours of various staged limb buds between mice and *D. sagitta*. We found that when scaled for size, the forelimbs of mice and three-toed jerboas are consistently identical in morphology. In contrast, the *D. sagitta* hindlimb starts to be noticeably narrower as early as 11.5 days post conception (dpc) (Extended Data Fig. 2).

Accordingly, we conducted an expression screen of a series of genes known to be involved in limb patterning just before and at the time of morphological divergence in hindlimb bud shape. None of the patterning genes we examined showed an obvious difference in expression in the *D. sagitta* hindlimb, including *Shh*, *Ptch1, Gli1* and *HoxD13* (Fig. 2a, b). Turning to post-patterning stages, cell proliferation was assessed by phospho-histone H3 antigen detection. However, we did not see a decrease in proliferation in the hindlimb of the three-toed jerboa, either at early stages of autopod expansion or later during digit outgrowth in any domain of the developing limbs (Extended Data Fig. 3). In contrast, we saw derived expanded domains of TdT-mediated dUTP nick end labelling (TUNEL)-positive nuclei, a marker for programmed cell death, specific to the jerboa hindlimb as early as 12.5 dpc (Extended Data Fig. 6). These domains further expand by 13.5 dpc to encompass all of the tissue distal to what would become the truncated cartilage condensations (Fig. 3b). Thus

[1]Department of Genetics, Harvard Medical School, Boston, Massachusetts 02115, USA. [2]Department of Animal Biology, University of Illinois Urbana-Champaign, Urbana, Illinois 61801, USA. [3]École Normale Supérieure de Lyon, 69007 Lyon, France. [4]Department of Molecular Biology and Genetics, Cornell University, Ithaca, New York 14853, USA. [5]The Camel Reproduction Centre, Dubai, United Arab Emirates. †Present address: Division of Biological Sciences, University of California, San Diego, La Jolla, California 92093, USA.
*These authors contributed equally to this work.

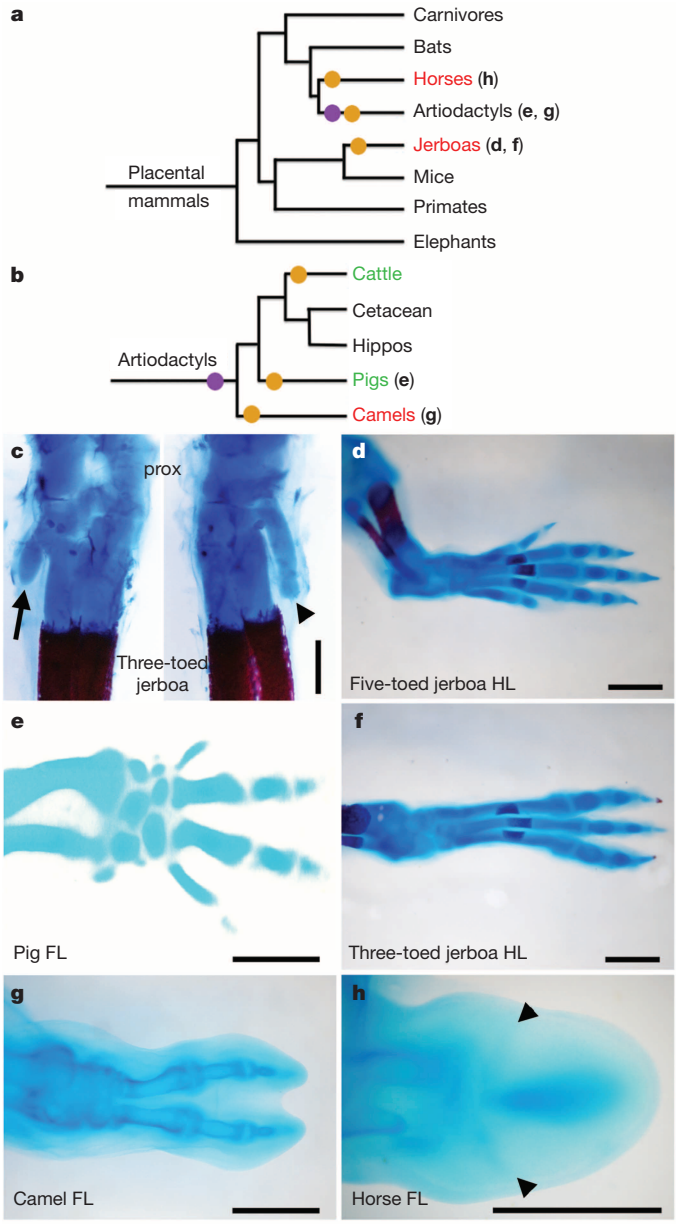

Figure 1 | Convergent evolution of the embryonic limb skeleton in multiple mammal species. **a**, **b**, Phylogeny of mammals (**a**) and of artiodactyls (**b**) representing the major groups that have independently lost digits, based on ref. 37. Parenthetical lettering references skeletons in accompanying panels. Orange circles indicate an evolutionary incidence of digit loss. Purple circles represent the shift from mesaxonic to paraxonic limbs in basal artiodactyls. Species that sculpt the limb by cell death are highlighted in red, and those that show a restriction of *Ptch1* expression are highlighted in green. **c,** Alcian blue and alizarin red stained skeleton of postnatal day 0 three-toed jerboa, *D. sagitta,* with the ankle (proximal) at the top. Posterior view (left) highlights the truncated fifth metatarsal (arrow). Anterior view (right) highlights the truncated first metatarsal (arrowhead) ($n = 4$ embryos). **d**, Alcian blue stained skeletons of the approximately 16 dpc five-toed jerboa, *A. elater,* hindlimb (HL) ($n = 3$ embryos). **e**, 30 dpc pig forelimb (FL) ($n = 2$ embryos). **f**, Approximately 16 dpc *D. sagitta* hindlimb ($n = 2$ embryos). **g**, 50 dpc camel hindlimb ($n = 1$ embryos). **h**, 34 dpc horse forelimb ($n = 1$ embryo). Scale bar, 0.5 mm. (**c**, **d**, **f**); scale bar, 1 mm (**e**, **g**, **h**).

digit loss in this species appears to result from the sculpting of anterior (pre-axial) and posterior (post-axial) tissues at the distal ends of properly patterned nascent digits.

Apoptosis is used in basal tetrapods to sculpt the digits, removing interdigital tissue late in limb development[12]. This suggests that a

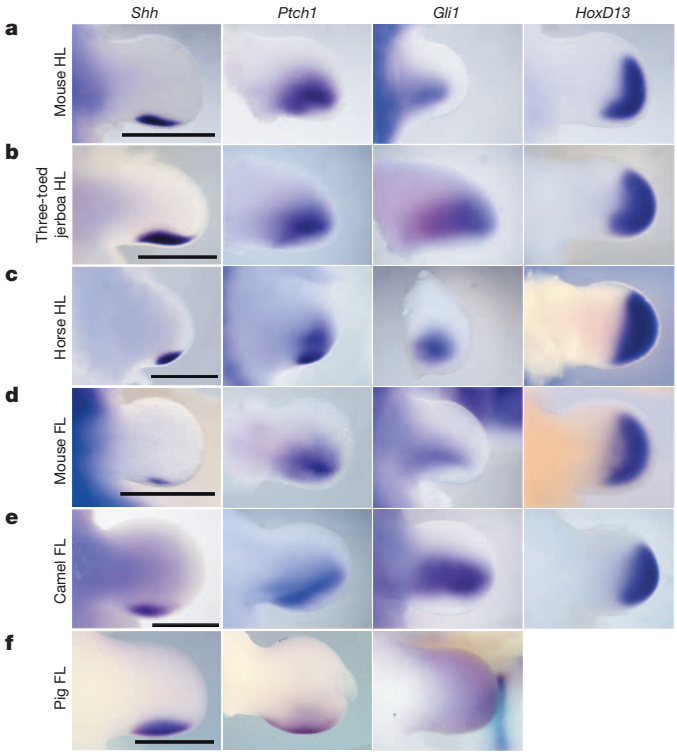

Figure 2 | Expression of early patterning genes: *Shh, Ptch1, Gli1* and *HoxD13*. **a**, Mouse hindlimb ($n = 3$ embryos per gene). **b**, Three-toed jerboa, *D. sagitta,* hindlimb ($n = 3$ embryos per gene). **c**, Horse hindlimb ($n = 1$ embryo for *Shh* and $n = 2$ embryos for *Ptch1, Gli1*, and *HoxD13*). **d**, Mouse forelimb ($n = 3$ embryos per gene). **e**, Camel forelimb ($n = 1$ each for *Shh* and *HoxD13* and $n = 2$ embryos for *Ptch1* and *Gli1*). **f**, Pig forelimb. Scale bar, 1 mm.

potential evolutionary route for achieving cell death in the *D. sagitta* hindlimb digit I and V primordia might be through co-option of the apoptotic pathways normally used to direct interdigital cell death. The transcription factor *Msx2* is strongly expressed in the interdigital tissue of the embryonic mouse and chicken[13], and retroviral misexpression in chicken embryos induces a striking increase in cell death and loss of cartilaginous digit condensations[14,15]. We found that *Msx2* is strongly expressed in the *D. sagitta* hindlimb in tissue surrounding and distal to the truncated first and fifth metatarsals and completely overlaps with domains of TUNEL-positive nuclei (Fig. 4a–c). In different contexts within the limb bud, the secreted protein *Bmp4* can act both upstream and downstream of *Msx2*[15,16]. We observe a transient spatial increase of *Bmp4* expression specific to the *D. sagitta* hindlimb autopod starting at 12 dpc that resolves at 12.5 dpc into two strong and discrete domains of expression precisely prefiguring the proximal positions of the first and fifth digits (Extended Data Fig. 4). However, *Msx2* is expanded in the *D. sagitta* hindlimb before expanded *Bmp4* expression, as early as 11 dpc (Extended Data Fig. 5). This is when the *D. sagitta* hindlimb first shows signs of narrowing relative to limbs that will develop five digits (Extended Data Fig. 2), consistent with altered *Msx2* expression potentially being the primary causal mechanism of digit loss in this species.

As the interdigital tissue begins to undergo apoptosis during mouse limb development, *Fgf8* expression is lost in the overlying apical ectodermal ridge (AER), whereas *Fgf8* expression is maintained above the growing digits (Fig. 5a). *Fgf8* is both necessary and sufficient for digit outgrowth in mouse and chicken embryos[17–20]. From about 12.75 dpc in the *D. sagitta* hindlimb, *Fgf8* expression regresses away from the posterior and then anterior AER as well as the interdigital domains, persisting only over the digits that continue to develop to completion (Fig. 5a, b and Extended Data Fig. 6).

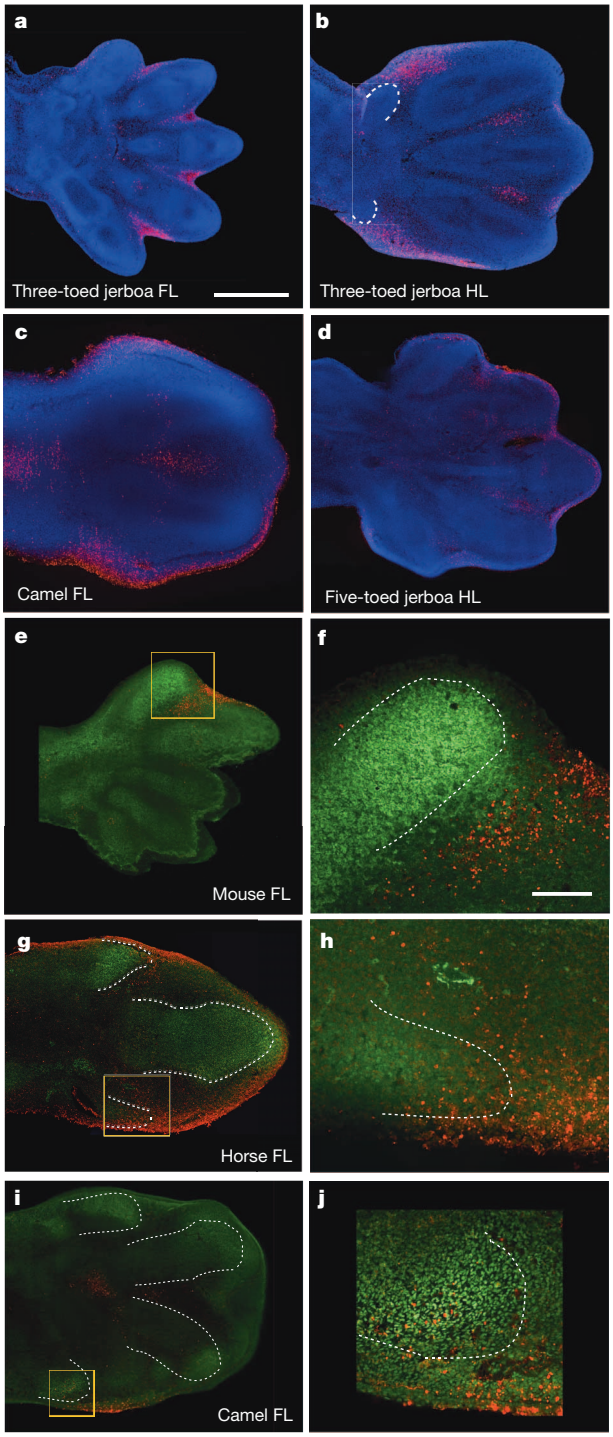

Figure 3 | Patterns of cell death in each mammalian limb. Fluorescent detection of DAPI (4′,6-diamidino-2-phenylindole) is blue, Sox9 immunohistochemistry is green, and TUNEL is red. **a**, Approximately 13.5 dpc three-toed jerboa, *D. sagitta,* forelimb. **b**, Approximately 13.5 dpc *D. sagitta* hindlimb (white dashed line indicates truncated metatarsals I and V) ($n = 2$ embryos). **c**, 45 dpc camel forelimb ($n = 1$ embryo). **d**, Approximately 13.5 dpc five-toed jerboa, *A. elater,* hindlimb ($n = 2$ embryos). **e**, Mouse at 13.5 dpc with Sox9 and TUNEL ($n = 3$ embryos). **f**, Magnification of boxed region in (**e**). **g**, 34 dpc horse forelimb ($n = 3$ embryos). **h**, Magnification of boxed region in (**g**). **i**, 42 dpc camel forelimb ($n = 2$ embryos). **j**, Magnification of boxed region in (**i**). Scale bar, 0.5 mm in **a** is also the same for **b**–**d**, **e**, **g** and **i**. Scale bar, 0.1 mm in **f** is also the same for **h** and **j**.

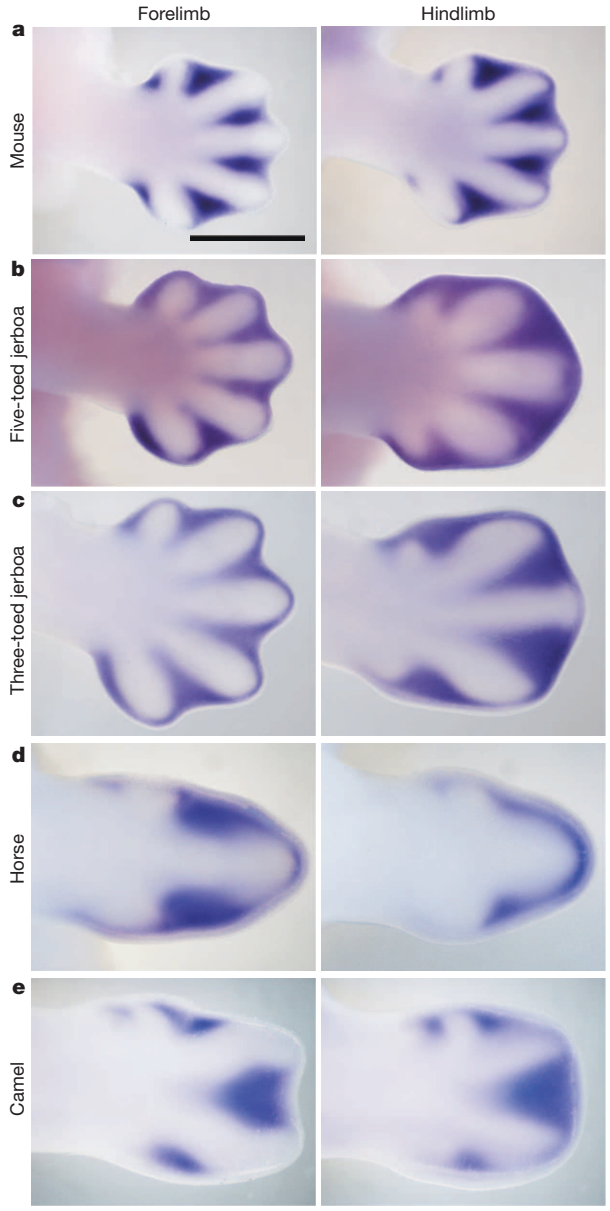

Figure 4 | Expression of *Msx2* at the start of digit chondrogenesis. **a**–**e**, Forelimb and hindlimb of 13 dpc mouse ($n = 3$ embryos) (**a**); approximately 13 dpc five-toed jerboa, *A. elater* ($n = 2$ embryos) (**b**); approximately 13 dpc three-toed jerboa, *D. sagitta* ($n = 2$ embryos) (**c**); 34 dpc horse ($n = 2$ embryos) (**d**); 42 dpc camel ($n = 1$ embryo) (**e**). Scale bar, 1 mm.

Convergence of post-pattern sculpting in the horse

The three-toed jerboa hindlimb remarkably resembles the limb structure of some of the early ancestral equine species with three toes[21]. To test possible mechanisms for digit reduction in the horse, we once again started by examining the expression of genes known to be involved in patterning the early limb bud. We observed no obvious differences in expression of *Shh, Ptch1*, *Gli1* or *HoxD13* relative to those previously described in mice (Fig. 2c). In contrast, we did observe TUNEL-positive nuclei entirely surrounding the central toe and within the distal ends of nascent $Sox9^{+}$ truncated condensations of metacarpals 2 and 4 (Fig. 3g, h), a condition not observed in mouse (Fig. 3e, f). Moreover, we found expanded *Msx2* expression in domains correlating with those regions of anterior and posterior cell death (Fig. 4d). We also observed increased posterior expression of *Msx2* earlier in development (Extended Data Fig. 5) and distal expansion of *Bmp4* in both forelimbs and hindlimbs (Extended Data Fig. 4) similar to *D. sagitta* hindlimbs. *Fgf8* expression is

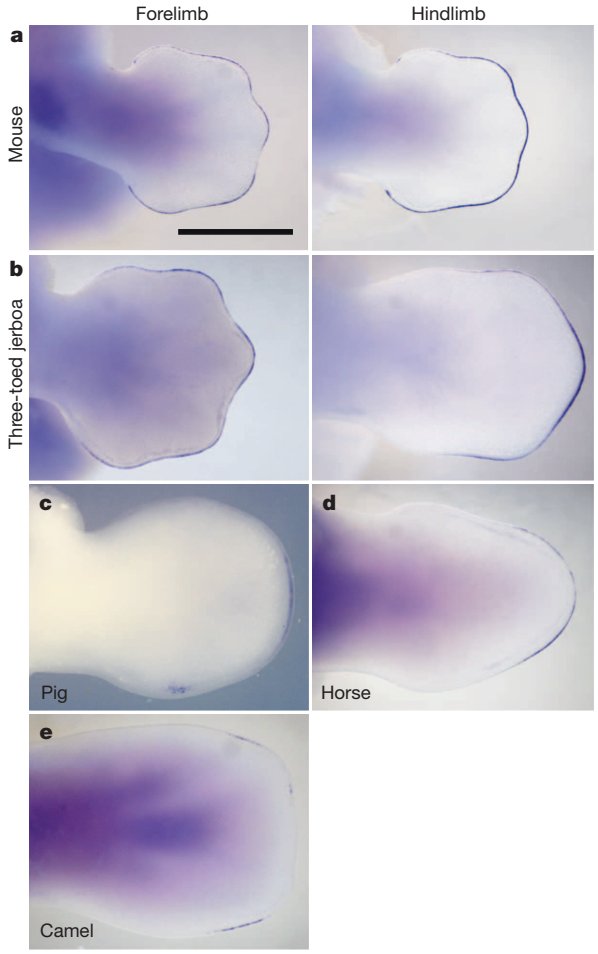

Figure 5 | *Fgf8* expression is restricted to the AER overlying nascent digits. **a**–**e**, Forelimb and hindlimb of 13 dpc mouse ($n = 3$ embryos) (**a**); approximately 13 dpc three-toed jerboa, *D. sagitta* ($n = 3$ embryos) (**b**); 25 dpc pig ($n = 2$ embryos) (**c**); 34 dpc horse hindlimb ($n = 2$ embryos) (**d**); 42 dpc camel forelimb ($n = 1$ embryo) (**e**). Scale bar, 1 mm.

also maintained in the horse AER only over the nascent central digit III (Fig. 5d). Thus, in the horse as in the three-toed jerboa, digit reduction appears to have a post-patterning contribution involving expanded domains of lateral apoptosis, possibly in part through similar molecular mechanisms. It is probable that mechanisms yet to be identified eliminate the first and fifth digits while a jerboa-like carving away of digits II and IV occurs by transforming cells from a chondrogenic to an apoptotic fate. A more extensive investigation of early patterning may be worthwhile with additional precisely staged early horse embryos.

Plasticity in artiodactyl digit loss

The even-toed ungulates present yet another opportunity to explore the possible convergence of digit reduction mechanisms in the context of additional skeletal remodelling. The distal artiodactyl limb has shifted the central axis of symmetry from digit III in the ancestral mesaxonic limb to a derived paraxonic limb where the axis of symmetry runs through the interdigital space between digits III and IV[22]. To explore whether digit loss in these species occurs via patterning and/or post-patterning changes, we obtained embryos from two species of artiodactyls, the pig and camel. While this work was in progress, we learned of similar studies by Lopez-Rios *et al.*[23] in a third artiodactyl species with convergent digit loss to two toes, the cow. The accompanying paper[23] identifies a gene regulatory control region for *Ptch1* expression in the limb that is altered in the cow. The resulting expression of *Ptch1* is reduced and more posteriorly restricted than in non-artiodactyl species. One role that *Ptch1* expression serves is to restrict the movement of the morphogen *Shh* across the limb bud[24,25]. As a consequence of the change in *Ptch1* expression in the cow, *Shh* targets, including *Gli1* and the *Hoxd* genes, are expressed more uniformly across the limb bud[23]. Mice in which *Ptch1* expression is reduced in the limb display similar changes in downstream genes and a concomitant shift in the central axis of the limb to the space between digits III and IV and loss of the first digit[26]. Importantly, after learning of our results with the three-toed jerboa and horse, Lopez-Rios and colleagues looked closely and saw no evidence of expanded apoptosis in the developing cow limb[23]. Together these results suggest that, as in *Hemiergis,* the even-toed ungulates might have lost digits through a *Shh*-dependent patterning mechanism, albeit by a different genetic alteration, allowing the digits to be lost in an asymmetrical manner in the artiodactyls.

As would be expected if mutations affecting *Ptch1* regulation play a prominent role in artiodactyl limb evolution, we find *Ptch1* expression in the pig is also posteriorly restricted and downregulated concomitant with an upregulation of *Gli1* (Fig. 2f). Furthermore, as in the cow, there is no evidence of increased cell death in developing pig limbs[27]. Surprisingly, however, *Ptch1* expression is not downregulated and restricted in the camel and is instead expressed much like non-artiodactyls (Fig. 2e). In addition, *Shh*, *Gli1,* and *HoxD13* exhibit ancestral patterns of expression indicating early patterning of the digit field by this subset of molecules is conserved in the camel (Fig. 2e). In contrast, when we examined patterns of cell death in the camel, we found expansive apoptosis throughout outgrowths of tissue flanking digits III and IV at 45 dpc (Fig. 3c) as well as at 42 dpc within small $Sox9^{+}$ pre-cartilaginous nodules in the positions of missing digits II and V (Fig. 3i, j). As in the three-toed jerboa and horse, this correlates with domains of *Msx2* expression in the anterior and posterior limb bud at the time of digit condensation (Fig. 4e), though earlier expression of *Bmp4* and *Msx2* does not correlate, suggesting a distinct initiating mechanism for camel (Extended Data Figs 4 and 5).

Regardless of the mechanism by which digit loss occurs, at patterning or post-patterning stages, *Fgf8* expression is lost from the AER anterior and posterior to the digits that continue to develop in the pig, camel (Fig. 5c, e), and cow[23], as seen with the three-toed jerboa and horse. Loss of *Fgf8* from the anterior and posterior AER in the pig and cow, two species that lack expanded domains of cell death, uncouples this expression change from the direct cause of apoptosis and may instead reflect an independent requirement for its elimination to allow for digit termination in all species.

Discussion

These data indicate that at least two mechanisms of digit reduction are employed in the even-toed ungulates, one (exemplified by the pig and cow) involving changes in early patterning by *Shh* and not involving apoptosis, and a distinct mechanism (seen in camels) involving changes in domains of apoptosis that resculpt the limb after the patterning phase. These data do, however, present a paradox in the context of the well-established artiodactyl phylogeny and fossil record (Fig. 1b). Although the morphology of the cow and pig is remarkably similar to the mouse phenotype when *Ptch1* is lost from the limbs, both in the reduction of digits and shift in the symmetry of toes to the interdigit of III–IV[23], it can not have been responsible for both phenotypes in the artiodactyls as they occurred at different stages evolutionarily. The change in *Ptch1* regulation seen in both pigs and cattle indicates that it was probably present in their last common ancestor. As such, it cannot have been solely responsible for the loss of digit 1, as this occurred convergently in these two lineages. Indeed, digit reduction occurred at multiple independent times within the artiodactyl clade (Fig. 1b, orange circles), as the stem group of each major lineage was pentadactyl at least in the forelimb[28]. The common ancestor of pigs and cattle would also have been ancestral to the hippos and their cetacean relatives, the dolphins and whales (Fig. 1b). Like extinct basal artiodactyls, hippos and basal cetaceans have a relatively small first digit[22,27,29]. Thus, a restriction of *Ptch1* in a basal member of the group including pigs, hippos, cetaceans, and cattle may have served to reduce the size of the first digit and predispose the limb to further digit loss.

Perhaps even more striking is the absence of altered *Ptch1* regulation in the camel. Without this information, one might have speculated that the

Ptch1 mutation was responsible for the reorientation of the axis of symmetry in artiodactyls similar to the mutant mouse. However, the shift in the position of digits from mesaxonic to paraxonic is believed to be ancestral to the split of modern artiodactyl suborders (and indeed is a defining characteristic trait for this clade[30–32]) (Fig. 1b, purple circle). Given the camel evidence, one has to either conclude that the shift actually arose independently in the ancestors of the camels and those of other artiodactyl lineages, or alternatively, any role *Ptch1* may have in the establishment of digit position in the pig and cow arose secondary to a separate mechanism established before the split of camels and their relatives.

The identification of several distinct molecular and cellular mechanisms of digit loss with recurring motifs suggests the developmental program of the tetrapod limb is fairly plastic. This would have provided some flexibility to allow adaptation in different circumstances and ultimately contributed to the diversity of limbs seen today.

METHODS SUMMARY

All embryos were collected in accordance with the appropriate Institutional Animal Care and Use Committee guidelines. Skeletal stainings were performed as previously described[33,34]. Whole mount *in situ* hybridizations were performed for mouse, three and five-toed jerboa, horse, and camel as in ref. 35 and for pig embryos as in ref. 36. Riboprobes were generated by PCR amplifying from cDNA of the appropriate species, cloning into pGEM-T-Easy (Promega), sequence verification, and expression testing first in mouse embryos. Primers used for probe generation and accession numbers are listed in Extended Data Table 1. For TUNEL and immunohistochemistry (IHC), embryos were embedded in paraffin or gelatin and sectioned at 12 or 80 μm thickness. TUNEL was performed using the TMRed *In situ* Cell Death Detection Kit (Roche). Sox9 and PH3 IHC were each performed after boiling antigen retrieval in citrate buffer using a 1:500 dilution of rabbit anti-Sox9 (Millipore AB5535) or 1:200 dilution of rabbit anti PH3 (Cell Signal #9701) followed by a Cy2 or Alexa594 conjugated secondary respectively. Each experiment was performed in at least two limb buds (1–2 embryos per experiment). Fluorescent images were captured by confocal microscopy, and images of sequential sections were overlaid in NIH ImageJ.

Online Content Methods, along with any additional Extended Data display items and Source Data, are available in the online version of the paper; references unique to these sections appear only in the online paper.

Received 16 December 2013; accepted 22 May 2014.
Published online 18 June 2014.

1. Lande, R. Evolutionary mechanisms of limb loss in tetrapods. *Evolution* **32,** 73–92 (1978).
2. Skinner, A., Lee, M. S. & Hutchinson, M. N. Rapid and repeated limb loss in a clade of scincid lizards. *BMC Evol. Biol.* **8,** 310 (2008).
3. Shapiro, M. D. Developmental morphology of limb reduction in *Hemiergis* (squamata: scincidae): chondrogenesis, osteogenesis, and heterochrony. *J. Morphol.* **254,** 211–231 (2002).
4. Shapiro, M. D., Hanken, J. & Rosenthal, N. Developmental basis of evolutionary digit loss in the Australian lizard *Hemiergis*. *J. Exp. Zool. B Mol. Dev. Evol.* **297B,** 48–56 (2003).
5. Harfe, B. D. *et al.* Evidence for an expansion-based temporal Shh gradient in specifying vertebrate digit identities. *Cell* **118,** 517–528 (2004).
6. Towers, M., Mahood, R., Yin, Y. & Tickle, C. Integration of growth and specification in chick wing digit-patterning. *Nature* **452,** 882–886 (2008).
7. Zhu, J. *et al.* Uncoupling Sonic hedgehog control of pattern and expansion of the developing limb bud. *Dev. Cell* **14,** 624–632 (2008).
8. Alberch, P. & Gale, E. A. Size dependence during the development of the amphibian foot. Colchicine-induced digital loss and reduction. *J. Embryol. Exp. Morphol.* **76,** 177–197 (1983).
9. Walker, E. P. *Mammals of the World* (John Hopkins Press, 1964).
10. Shenbrot, G. I., Sokolov, V. E. & Heptner, V. G. *Jerboas: Mammals of Russia and Adjacent Regions* (Science Publishers, 2008).
11. Cooper, K. L. The lesser Egyptian jerboa, *Jaculus jaculus*: a unique rodent model for evolution and development. *Cold Spring Harb. Protoc.* **2011,** pdb.emo066704 (2011).
12. Zuzarte-Luis, V. & Hurle, J. M. Programmed cell death in the embryonic vertebrate limb. *Semin. Cell Dev. Biol.* **16,** 261–269 (2005).
13. Fernández-Terán, M. A., Hinchliffe, J. R. & Ros, M. A. Birth and death of cells in limb development: a mapping study. *Dev. Dyn.* **235,** 2521–2537 (2006).
14. Marazzi, G., Wang, Y. & Sassoon, D. Msx2 is a transcriptional regulator in the BMP4-mediated programmed cell death pathway. *Dev. Biol.* **186,** 127–138 (1997).
15. Ferrari, D. *et al.* Ectopic expression of Msx-2 in posterior limb bud mesoderm impairs limb morphogenesis while inducing BMP-4 expression, inhibiting cell proliferation, and promoting apoptosis. *Dev. Biol.* **197,** 12–24 (1998).
16. Pizette, S., Abate-Shen, C. & Niswander, L. BMP controls proximodistal outgrowth, via induction of the apical ectodermal ridge, and dorsoventral patterning in the vertebrate limb. *Development* **128,** 4463–4474 (2001).
17. Lewandoski, M., Sun, X. & Martin, G. R. Fgf8 signalling from the AER is essential for normal limb development. *Nature Genet.* **26,** 460–463 (2000). .
18. Mariani, F. V., Ahn, C. P. & Martin, G. R. Genetic evidence that FGFs have an instructive role in limb proximal-distal patterning. *Nature* **453,** 401–405 (2008).
19. Sun, X., Mariani, F. V. & Martin, G. R. Functions of FGF signalling from the apical ectodermal ridge in limb development. *Nature* **418,** 501–508 (2002).
20. Sanz-Ezquerro, J. J. & Tickle, C. Fgf signaling controls the number of phalanges and tip formation in developing digits. *Curr. Biol.* **13,** 1830–1836 (2003).
21. Romer, A. S. *Vertebrate Paleontology* (Univ. Chicago Press, 1936).
22. Prothero, D. R. & Foss, S. E. *The Evolution of Artiodactyls* (John Hopkins Univ. Press, 2007).
23. Lopez-Rios, J. *et al.* Attenuated sensing of SHH by Ptch1 underlies adaptive evolution of bovine limbs. *Nature* http://dx.doi.org/10.1038/nature13289 (this issue).
24. Chen, Y. & Struhl, G. Dual roles for Patched in sequestering and transducing Hedgehog. *Cell* **87,** 553–563 (1996).
25. Li, Y., Zhang, H., Litingtung, Y. & Chiang, C. Cholesterol modification restricts the spread of Shh gradient in the limb bud. *Proc. Natl Acad. Sci. USA* **103,** 6548–6553 (2006).
26. Butterfield, N. C. *et al.* Patched 1 is a crucial determinant of asymmetry and digit number in the vertebrate limb. *Development* **136,** 3515–3524 (2009).
27. Sears, K. E. *et al.* Developmental basis of mammalian digit reduction: a case study in pigs. *Evol. Dev.* **13,** 533–541 (2011).
28. Clifford, A. B. The evolution of the unguligrade manus in artiodactyls. *J. Vertebr. Paleontol.* **30,** 1827–1839 (2010).
29. Cooper, L. N., Berta, A., Dawson, S. D. & Reidenberg, J. S. Evolution of hyperphalangy and digit reduction in the cetacean manus. *Anat. Rec. Adv. Integr. Anat. Evol. Biol.* **290,** 654–672 (2007).
30. Rose, K. D. Skeleton of *Diacodexis*, oldest known artiodactyl. *Science* **216,** 621–623 (1982).
31. Rose, K. D. On the origin of the order Artiodactyla. *Proc. Natl Acad. Sci. USA* **93,** 1705–1709 (1996).
32. Theodor, J., Erfurt, J. & Metais, G. The earliest Artiodactyls: Diacodexeidae, Dichobunidae, Homacodontidae, Leptochoeridae, and Raoellidae in *The Evolution of Artiodactyls* (eds. Prothero, D.R. & Foss, S.E.) (John Hopkins Univ. Press, 2007).
33. Rasweiler, J. J., Cretekos, C. J. & Behringer, R. R. Alcian blue staining of cartilage of short-tailed fruit bat (*Carollia perspicillata*). *Cold Spring Harb. Protoc.* **2009,** pdb.prot5165 (2009).
34. Ovchinnikov, D. Alcian blue/alizarin red staining of cartilage and bone in mouse. *Cold Spring Harb. Protoc.* **2009,** pdb.prot5170 (2009).
35. Riddle, R. D., Johnson, R. L., Laufer, E. & Tabin, C. Sonic hedgehog mediates the polarizing activity of the ZPA. *Cell* **75,** 1401–1416 (1993).
36. Rasweiler, J. J., Cretekos, C. J. & Behringer, R. R. Whole-mount *in situ* hybridization of short-tailed fruit bat (*Carollia perspicillata*) embryos with RNA probes. *Cold Spring Harb. Protoc.* **2009,** pdb.prot5164 (2009).
37. Meredith, R. W. *et al.* Impacts of the Cretaceous terrestrial revolution and KPg extinction on mammal diversification. *Science* **334,** 521–524 (2011).

Acknowledgements We thank J. Lopez-Rios and R. Zeller (University of Basel, Switzerland) for generously providing data and discussion before publication. We also thank J. Carlos Izpisua Belmonte and A. Aguirre for sharing space and materials to complete experiments subsequent to review. Jerboa embryos were harvested with the assistance of S. Wu and colleagues in Xinjiang, China. Pig embryos were harvested with the assistance of D. Urban. Additional horse embryos were provided by R. Turner and H. Galatino-Homer (University of Pennsylvania) and by R. Fritsche and S. Lyle (Louisiana State University). Mouse *Gli1* probe plasmid, used in the pig *in situ*, was provided by A. Joyner. This work was supported by NIH grant R37HD032443 to C.J.T., and NSF IOS grant 1257873 to K.E.S.

Author Contributions K.L.C., K.E.S. and C.J.T. conceived of and initiated the project. K.L.C. and C.J.T. wrote the manuscript. K.L.C performed the mouse, three- and five-toed jerboa, horse and camel *in situ* hybridizations, PH3 IHC, and skeletal stains. A.U. performed TUNEL and Sox9 IHC. J.M. and K.E.S. performed the pig *in situ* hybridizations. K.-S.B. cloned the pig probes. M.B. and D.A. provided most of the horse embryos and material for cloning the horse probes. J.A.S. provided the camel embryos and material for cloning the camel probes.

Author Information The probe sequence data for all genes and species has been deposited in the NCBI Probes database with the following accession numbers: CAMELBMP4, Pr032067180; CAMELFGF8, Pr032067181; CAMELGLI1, Pr032067182; CAMELHOXD13, Pr032067183; CAMELPTCH1, Pr032067184; HORSEBMP4, Pr032067185; HORSEFGF8, Pr032067186; HORSEGLI1, Pr032067187; HORSEHOXD13, Pr032067188; HORSEMSX2, Pr032067189; HORSEPTCH1, Pr032067190; HORSESHH, Pr032067191; JERBOABMP4, Pr032067192; JERBOAFGF8, Pr032067193; JERBOAGLI1, Pr032067194; JERBOAHOXD13, Pr032067195; JERBOAMSX2, Pr032067196; JERBOAPTCH1, Pr032067197; JERBOASHH, Pr032067198; MOUSEBMP4, Pr032067199; MOUSEFGF8, Pr032067200; MOUSEGLI1, Pr032067201; MOUSEHOXD13, Pr032067202; MOUSEMSX2, Pr032067203; MOUSEPTCH1, Pr032067204; MOUSESHH, Pr032067205; PIGFGF8, Pr032067206; PIGPTCH1, Pr032067207; PIGSHH, Pr032067208. Reprints and permissions information is available at www.nature.com/reprints. The authors declare no competing financial interests. Readers are welcome to comment on the online version of the paper. Correspondence and requests for materials should be addressed to K.L.C. (kcooper@ucsd.edu); correspondence and requests for pig embryos and materials should be addressed to K.E.S. (ksears@life.illinois.edu).

METHODS

Samples

All embryos were collected in accordance with the appropriate Institutional Animal Care and Use Committee guidelines. Experiments were not randomized or blinded. The age and species of each specimen is noted in the figure legends. The sex of the embryos is unknown. Mouse embryos are of the CD-1 strain.

Skeletal preparation. For the mouse and jerboa samples, skeletal preparations were performed as previously described[34]. The embryos were eviscerated and fixed in 95% ethanol overnight and then in acetone overnight at room temperature. Embryos were subsequently stained overnight at room temperature in alcian/alizarin staining solution (5 ml each alcian blue and alizarin red S stock, 5 ml glacial acetic acid, 85 ml 70% ethanol). The alcian stock was: 0.3 g Alcian Blue 8GX (Sigma-Aldrich A5268) in 70% ethanol; the alizarin stock: 0.1 g Alizarin Red S (Sigma-Aldrich A5533), 5 ml H_2O, 95 ml absolute ethanol. Embryos were then cleared in 1% KOH that was replaced with fresh solution when it turned purple. When skeletal features were visible and soft tissues only slightly blue, embryos were carried through a graded series of 25%, 50%, 75% glycerol in 1% KOH and then into 100% glycerol for imaging and storage.

For the horse and camel samples, skeletal preparations were performed as previously described[33]. The embryos were fixed in 4% paraformaldehyde in 1× PBS and dehydrated through a graded methanol series into 100% methanol for storage at −20 °C. Embryos were then rehydrated to PBS and transferred to 0.1% ammonium hydroxide in 70% ethanol overnight to bleach. Embryos were then washed twice for an hour in acid alcohol (5% acetic acid, 70% ethanol). Staining was carried out for three hours at room temperature in 0.05% alcian blue, 5% acetic acid, 70% ethanol. Embryos were washed two times for an hour in acid alcohol, cleared in 100% methanol (two times for an hour) and then transferred to BABB (1:2 benzyl alcohol: benzyl benzoate) for further clearing, imaging and storage.

For the pig samples, limbs were removed from pig embryos and stored in 100% methanol. Skin was dissected off limbs and limbs were briefly rehydrated through a methanol series into 100% PBS. Limbs were then placed in alcian blue overnight (0.02% alcian blue in ethanol and 30% glacial acetic acid). The next day limbs were washed for an hour each in 100%, 95% and 70% ethanol, then washed with deionized water for 1 h. Limbs were stained with Alizarin red (0.1% in 1% KOH) overnight. The next day the limbs were cleared in 1% KOH and solution changed every day until skeletal features were visible. Limbs were moved to glycerol for extended preservation.

Whole-mount *in situ* hybridization. Mouse, jerboa, horse and camel *in situ* hybridizations were performed as in ref. 35. Pig *in situ* hybridizations were performed as in ref. 36. Probe templates for all species were generated by PCR from first strand cDNA synthesis (primers and accession numbers provided in Extended Data Table 1). PCR products were ligated into pGEM-T-Easy (Promega), transformed into DH5α competent cells, and plated for blue white selection on IPTG/XGal/Amp plates. White colonies were selected for sequence verification and then plasmid prepped (Qiagen). Plasmids were linearized with the appropriate restriction enzyme and then a transcription reaction was carried out using the appropriate anti-sense transcription enzyme (SP6 or T7) with digoxygenin RNA labelling mix (Roche). RNA probes were precipitated with LiCl2 and ethanol and resuspended in 50 µl nuclease-free water plus 1 µl RNase inhibitor. One microlitre of probe was run on an agarose gel to confirm probe synthesis.

All embryos for whole-mount *in situ* hybridization (WISH) were fixed with 4% paraformaldehyde in 1× PBS and dehydrated through a graded methanol series (25%, 50%, 75% MeOH in PBS, 100% MeOH) and stored at −20 ° C until use. Before WISH, embryos were treated with 6% H_2O_2 in methanol for 1 h, and rehydrated through a methanol series to PBST (PBS plus 0.1% Tween-20).

After three 5-min washes in PBST, proteinase K (10 µg ml^{-1} in PBST) was added and embryos were incubated at room temperature for 25 (21.5 to 22.5 dpc: pigs), 35 (22.5 to 23.5 dpc: pigs), or 45 (25.5 to 26.5 dpc: pigs) minutes. Mouse and jerboa embryos were permeabilized in 10 µg ml^{-1} proteinase K as follows: 11 dpc for 20 min, 11.5 dpc for 22 min, 12 dpc for 25 min, 12.5 dpc for 27 min, 13 dpc for 30 min. For *fgf8* WISH, embryos of all species were incubated in proteinase K for 10 min regardless of age. Camel and horse embryos in Fig. 2 were incubated for 30 min in proteinase K, camel and horse embryos in Fig. 4 for 45 min, and those in Extended Data Figs 4 and 5 for 40 min.

After permeablization, embryos were washed in PBST and then fixed for 20 min in 4% PFA/0.2% glutaraldehyde in PBST. After several washes with PBST, embryos were added to pre-warmed prehybridization solution (pig: 50% formamide, 5× SSC pH 4.5, 2% SDS, 2% Roche blocking reagent, 250 µg ml^{-1} tRNA, 100 µg ml^{-1} heparin sodium salt; other species: 50% formamide, 5× SSC pH 4.5, 1% SDS, 50 µg ml^{-1} yeast tRNA, 50 µg ml^{-1} heparin) and incubated for at least 1 h at 70 °C (pig) or 65 °C (other species). After pig embryo incubation, the pre-hybridization solution was changed to fresh with 1 µl probe added followed by overnight incubation at 70 °C. For other species, pre-hybridization solution was replaced with fresh solution containing 1:200 dilution of the appropriate probe followed by overnight incubation at 65 °C.

For pig samples, on day two, four 30-min washes in solution I (50% formamide, 2× SSC pH 4.5, 1% SDS) were performed at 70 °C. Embryos were then briefly washed at room temperature in a 50/50 mix of Solution I and MABT (100 mM maleic acid, 150 mM NaCl, 0.1% Tween-20, pH 7.5). Next, two 30-min washes were done in MABT. Embryos were then blocked in 2% blocking reagent/MABT for 1 hour. A final blocking step was done for at least 1 h in 20% heat inactivated goat serum/2% blocking reagent/MABT. Anti-DIG antibody (Roche) was added at 1:2,000 to fresh blocking solution and embryos incubated overnight at 4 °C. The next day embryos were washed all day (changing solution five times) and overnight in MABT. The following day embryos were washed in NTMT (100 mM NaCl, 100 mM Tris pH 9.5, 50 mM $MgCl_2$, 0.1% Tween-20) for four 10-min washes and then placed in a BM Purple solution (Roche). During their time in BM purple, samples were wrapped in foil and monitored for the appearance of staining. After the colour reaction had reached an appropriate level, embryos were rinsed several times in NTMT, then PBST, and then fixed with 4% PFA overnight. Embryos were transferred to 1% PFA for long-term storage.

For other species, on day two, embryos were washed three times for 30 min in solution I (50% formamide, 5× SSC pH 4.5, 1% SDS) at 65 °C followed by three times for 30 min in solution III (50% formamide, 2× SSC pH 4.5) at 65 °C. Embryos were then washed three times for 5 min in TBST (1× TBS plus 1% Tween 20) and blocked for one hour at room temperature in block solution (10% heat inactivated sheep serum and 0.1% Roche blocking reagent in TBST). Embryos were then incubated overnight at 4 °C in block solution plus 1:2,500 anti-digoxygenin AP antibody (Roche). On day three, embryos were washed three times for 5 min in TBST and then five times for at least an hour each in TBST followed by overnight at 4 °C in TBST. On day four, embryos were washed three times 10 min in NTMT (100 mM NaCl, 100 mM Tris pH 9.5, 50 mM $MgCl_2$, 1% Tween-20) before colouration in AP reaction mix (125 µg ml^{-1} BCIP and 250 µg ml^{-1} NBT in NTMT). Colouration was carried to completion in the dark. Embryos were then washed 10 min in NTMT followed by three times 10 min in TBST and finally overnight in TBST to reduce background and increase signal. Embryos were post-fixed in 4% paraformaldehyde for 30 min at room temperature and imaged and stored in 1% paraformaldehyde in 1× PBS.

Immunohistochemistry and TUNEL. Paraformaldehyde fixed embryos for paraffin sectioning were dehydrated through an ethanol series, cleared in xylenes, and infiltrated with paraffin for embedding and sectioning. Embryos for frozen sections were paraformaldehyde fixed, dehydrated through a graded series to 100% methanol for storage and subsequently rehydrated into PBST before transfer to 15% sucrose in 1× PBS. Limbs were then dissected from the embryos and embedded in gelatin solution (7.5% gelatin and 15% sucrose in PBS) in disposable cryomolds. Blocks were frozen and stored at −80 °C until cryosectioned.

Slides for immunohistochemistry were rinsed in xylenes to dewax and rehydrated through an ethanol series to PBS (for paraffin sections) or thawed (for frozen sections) and washed twice in PBS. All immunohistochemistry was carried out after antigen retrieval in 1:100 dilution citric acid antigen unmasking solution (Vector labs) by boiling for 2 min in the microwave followed by incubation at room temperature wrapped tightly in foil and then cooling to room temperature for 20 min at 4 °C. Slides were washed in PBS (or TBS for phosphor-antibodies) and then blocked in a solution of 5% heat inactivated goat serum, 0.1% TritonX-100, 0.02% SDS in PBS (or TBS). Primary antibody was added at a concentration of 1:500 for Sox9 (Millipore AB5535) or 1:200 for phospho histone H3 (Cell Signal #9701) and slides incubated overnight in a humidified chamber at 4 °C. On day 2, slides were washed three times in PBST (or TBST) and incubated at room temperature in secondary antibody (goat anti-rabbit Alexa 594, Life Technologies) diluted 1:250 in block plus 0.1 µg ml^{-1} DAPI. Slides were then washed three times 5 min in PBS (or TBS) and mounted in Fluoromount-G (Southern Biotech).

For TUNEL, slides were rehydrated or thawed, washed in PBS, and then permeabilized for 10 min in 5 µg ml^{-1} proteinase K in PBS followed by 5 min post-fix in 4% paraformaldehyde in PBS and three washes in PBS. Slides were then incubated in TUNEL reaction mixture (Roche *In situ* Cell Death Detection Kit, TM-Red) for 60 min at 37 °C, rinsed three times in PBS, and mounted in Prolong Gold. Slides that had been previously processed for Sox9 IHC were placed immediately into the TUNEL reaction mixture.

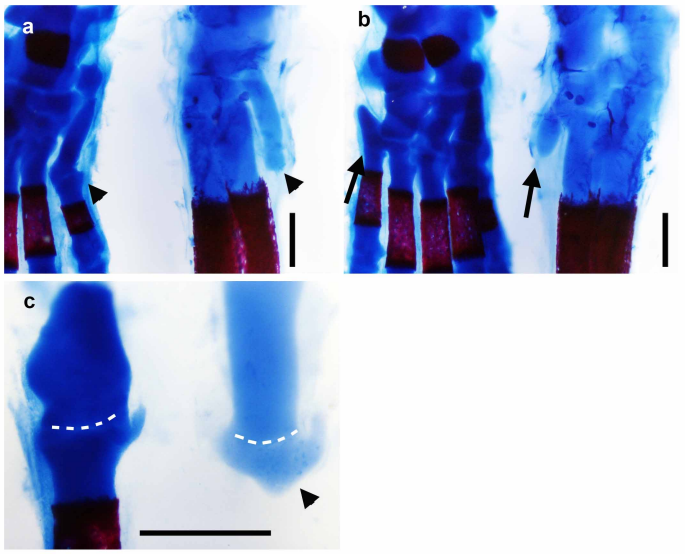

Extended Data Figure 1 | The proximal remnants of truncated skeletal elements in *D. sagitta* are correctly patterned. Alcian blue and alizarin red stained skeletons of postnatal day 0 mouse (left, $n = 4$ animals) and three-toed jerboa, *D. sagitta* (right, $n = 4$ animals) with proximal (ankle) at the top. **a**, Anterior view highlights the first metatarsal (arrowhead). **b**, Posterior view highlights the fifth metatarsal (arrow). **c**, Dissected first tarsal-metatarsal elements demonstrate the morphology of the truncated first metatarsal of *D. sagitta* (right, arrowhead) compared to mouse (left). Joint interzone indicated by white dashed line. Scale bars, 0.5 mm.

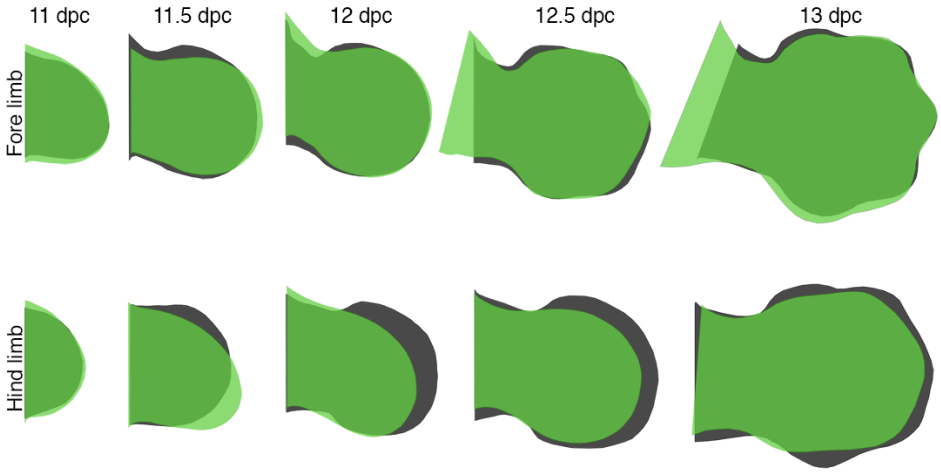

Extended Data Figure 2 | The shape of the three-toed jerboa hindlimb differs from the mouse as early as 11.5 dpc. Trace outlines of limb buds of the mouse (black) and three-toed jerboa, *D. sagitta* (green) over a developmental time series. Outlines are of embryos most representative of 3–4 individuals per stage.

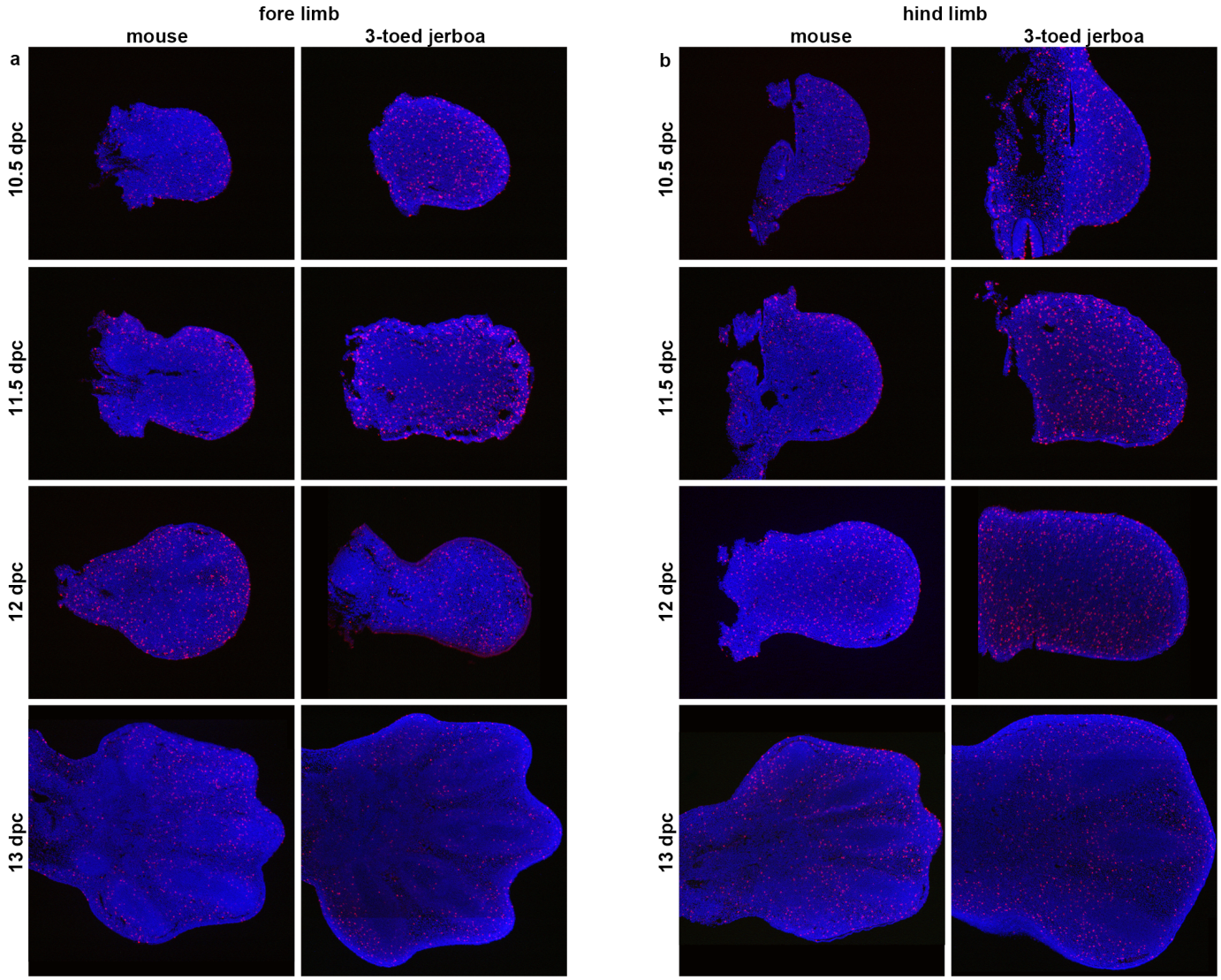

Extended Data Figure 3 | Proliferation is unchanged in the *D. sagitta* hindlimb bud. Phospho-histone H3 detection in sections of mouse and three-toed jerboa, *D. sagitta*, limb buds. **a**, Forelimbs. **b**, Hindlimbs. $n = 2$ embryos per stage and species.

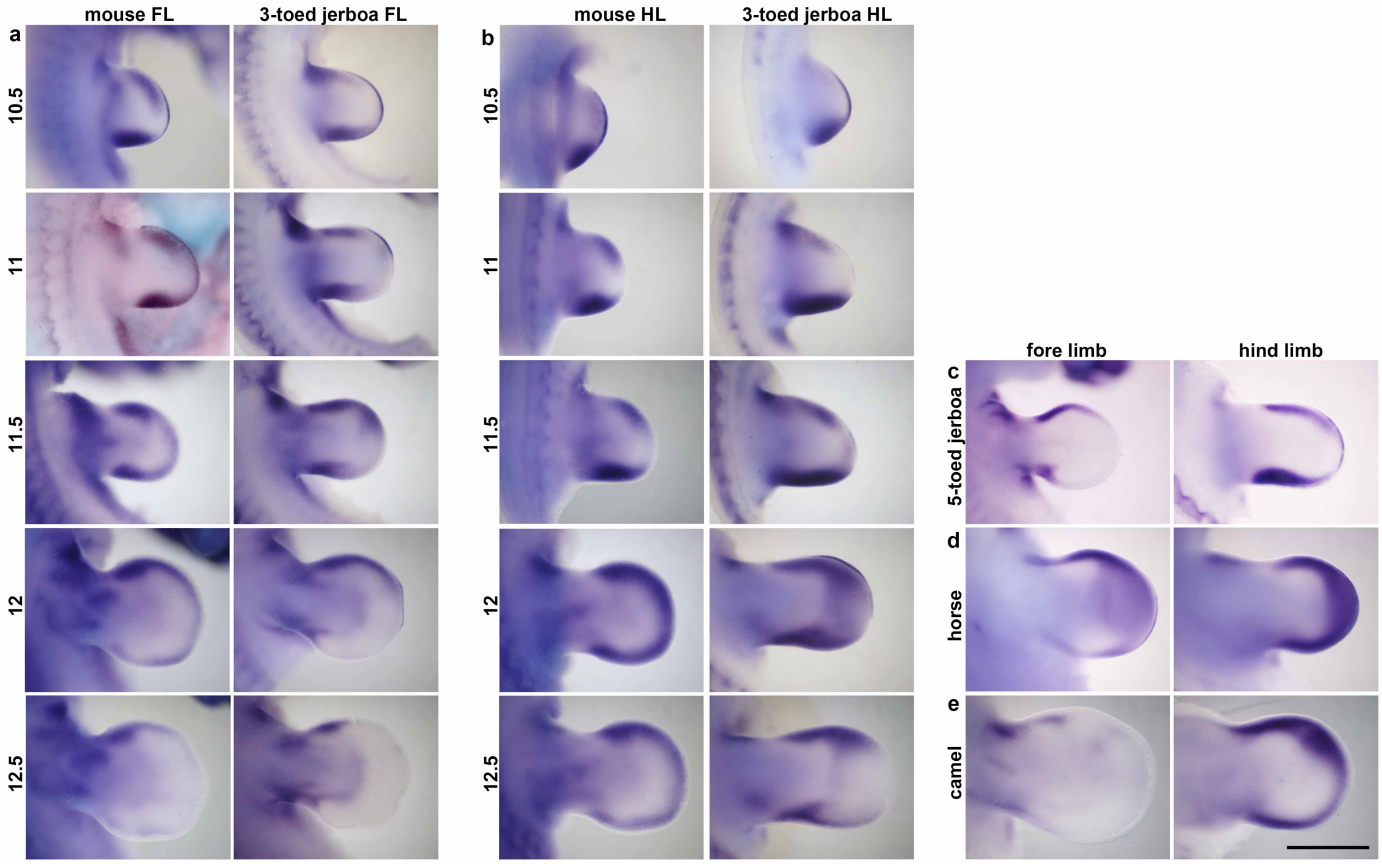

Extended Data Figure 4 | Developmental time course and species comparisons of *Bmp4* expression. **a**, **b**, Forelimb buds (FL) (**a**) and hindlimb buds (HL) (**b**) of mouse and the three-toed jerboa, *Dipus sagitta*, at 10.5, 11, 11.5, 12 and 12.5 dpc ($n = 2$ embryos per stage). **c**, Forelimb and hindlimb of the five-toed jerboa, *A. elater,* at approximately 12.25 dpc ($n = 1$ embryo). **d**, Forelimb and hindlimb of the horse at 30 dpc (approximately equivalent to mouse 12 dpc) ($n = 2$ embryos). **e**, Forelimb and hindlimb of the camel at 38 dpc (approximately equivalent to mouse 12.5 dpc) ($n = 1$ embryo). Scale bar, 1 mm for *D. sagitta, A. elater,* horse and camel. Scale bar, 0.8 mm for mouse limbs.

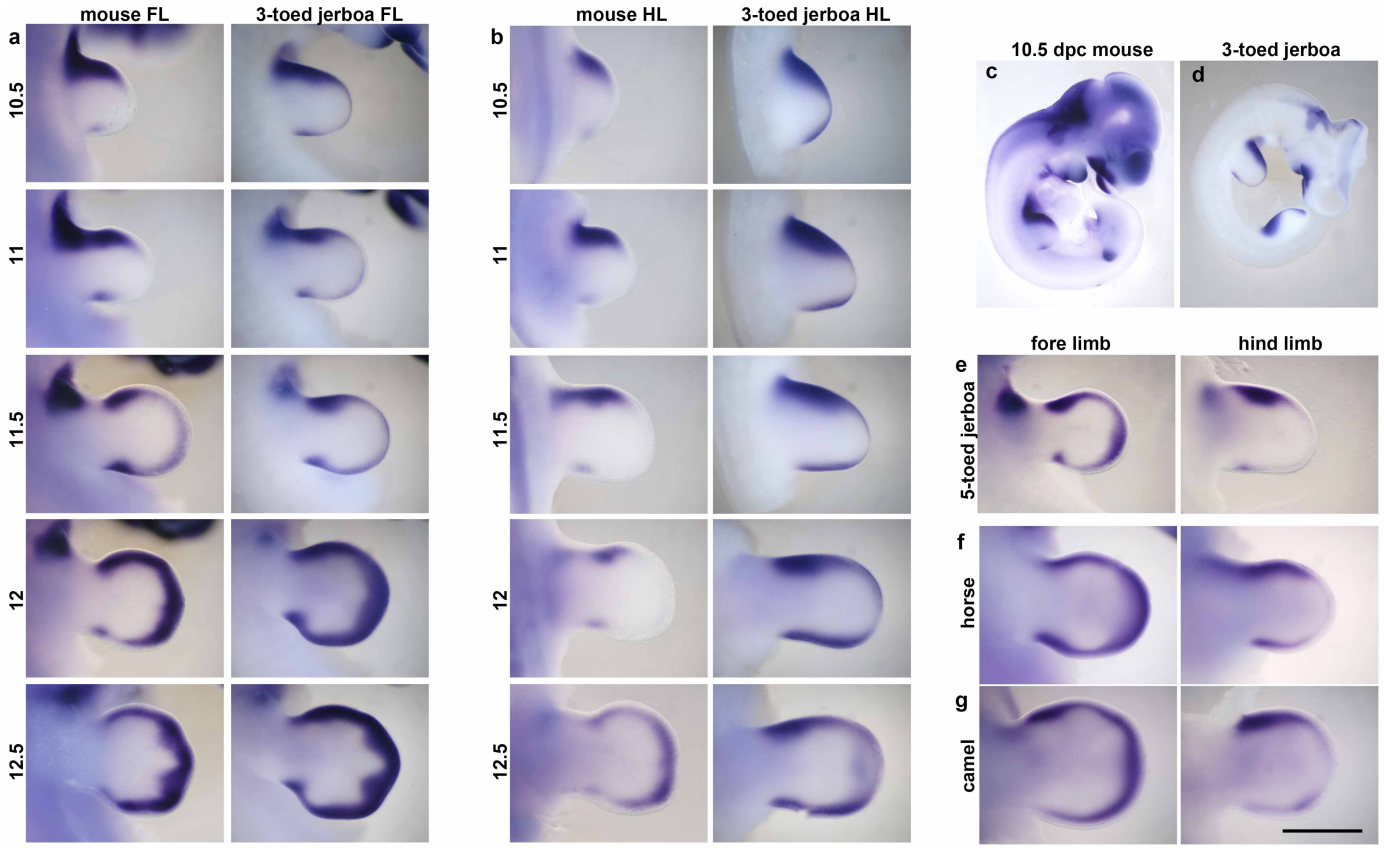

Extended Data Figure 5 | Developmental time course and species comparisons of *Msx2* expression. **a**, **b**, Forelimb buds (FL) (**a**) and hindlimb buds (HL) (**b**) of mouse and the three-toed jerboa, *D. sagitta*, at 10.5, 11, 11.5, 12 and 12.5 dpc ($n = 2$ embryos per stage). **c**, **d**, *Msx2* expression in the mouse (**c**) and *D. sagitta* (**d**) embryo at 10.5 dpc. **e**, Forelimb and hindlimb of the five-toed jerboa, *A. elater,* at approximately 12.25 dpc ($n = 1$ embryo). **f**, Forelimb and hindlimb of the horse at 30 dpc (approximately equivalent to mouse 12 dpc) ($n = 2$ embryos). **g**, Forelimb and hindlimb of the camel at 38 dpc (approximately equivalent to mouse 12.5 dpc) ($n = 1$ embryo). Scale bar, 1 mm for *D. sagitta, A. elater,* horse and camel. Scale bar, 0.8 mm for mouse limbs.

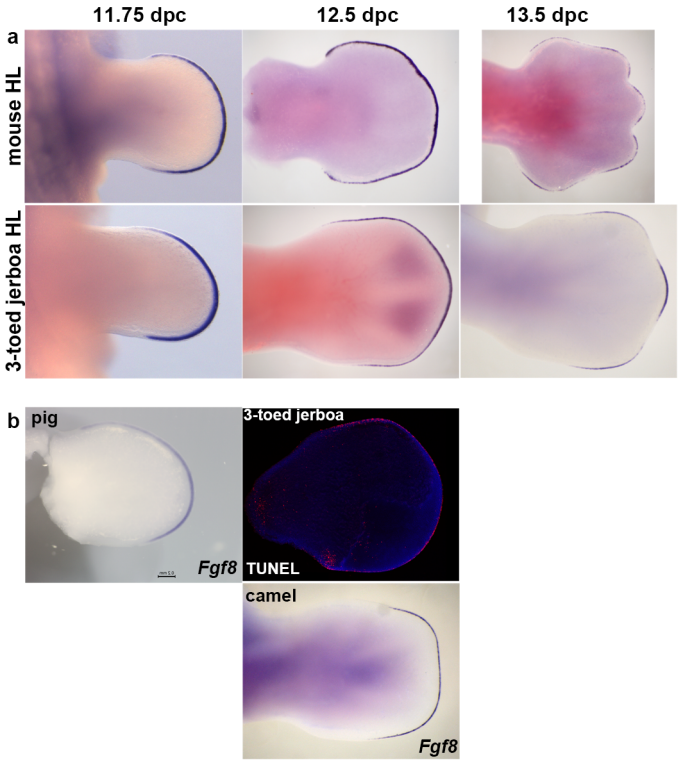

Extended Data Figure 6 | Developmental time course of *Fgf8* expression and early TUNEL in the jerboa hindlimb. **a**, Time series of *Fgf8* expression in the mouse and three-toed jerboa, *D. sagitta*, hindlimb ($n = 2$ embryos per stage). **b**, *Fgf8* expression in the pig (25 dpc) and camel (42 dpc) hindlimbs of embryos in Fig. 5. TUNEL labelling of cell death in the 12.5 dpc *D. sagitta* hindlimb ($n = 2$ embryos). Limbs in **b** are aligned with the closest stage matched embryos in **a**.

Extended Data Table 1 | Whole mount *in situ* hybridization probe information

Shh	Forward	Reverse	NCBI Accession #
mouse	GACCCCTTTAGCCTACAAGCAGTTT	GCGTCTCGATCACGTAGAAGACCT	Pr032067205
jerboa	GACCCCTTTAGCCTACAAGCAGTTT	GCGTCTCGATCACGTAGAAGACCT	Pr032067198
horse	CTGGTGGTTCTGGTCTCCTC	CCCTCGTCCGATCACGTA	Pr032067191
camel	used horse probe		
pig	CCGGCTGATGACTCAGAGAT	GCAGGTCCTTCACCAGCTT	Pr032067208
Ptch1			
mouse	CTTCGCTCTGGAGCAGATTT	GCATGGTTAAACAGGCATAGG	Pr032067204
jerboa	CTTCGCTCTGGAGCAGATTT	GCATGGTTAAACAGGCATAGG	Pr032067197
horse	CGCCAGAAGATTGGAGAAGA	CCTGAGTTGTTGCAGCGTTA	Pr032067190
camel	CGCCAGAAGATTGGAGAAGA	CCTGAGTTGTTGCAGCGTTA	Pr032067184
pig	GGAGCAGATTTCCAAGGGGA	CGGAGAGCTTCTGTGGTCAG	Pr032067207
Gli1			
mouse	TACATGCTGGTGGTGCACAT	GGCTGTGGCGAATAGACAGA	Pr032067201
jerboa	TACATGCTGGTGGTGCACAT	GGCTGTGGCGAATAGACAGA	Pr032067194
horse	GTGACCACTCCCCAGCAG	GATTCAGACCACTGCCCATC	Pr032067187
camel	TACATGCTGGTGGTGCACAT	GGCGGTCAAGAGAAACTGG	Pr032067182
Hoxd13			
mouse	CTATGGCTACCATTTCGGCAAC	ACTGGTAGCCCTCCATGGAAAT	Pr032067202
jerboa	CTATGGCTACCATTTCGGCAAC	ACTGGTAGCCCTCCATGGAAAT	Pr032067195
horse	TTCCCGGTGGAGAAGTACA	TTGAGCTTGGAGACGATTTTC	Pr032067188
camel	TTCCCGGTGGAGAAGTACA	TTGAGCTTGGAGACGATTTTC	Pr032067183
Msx2			
mouse	CTCTCGTCAAGCCCTTCGAGAC	AGCCATTTTCAGCTTTTCCAGTT	Pr032067203
jerboa	CTCTCGTCAAGCCCTTCGAGAC	AGCCATTTTCAGCTTTTCCAGTT	Pr032067196
horse	TCGCTTAGGGTGGTGTAAGC	TTGCTAATTCACCCCTCTCTG	Pr032067189
camel	used horse probe		
Bmp4			
mouse	AGTGAGAGCTCTGCTTTTCGTTTC	GGCAGTAGAAGGCCTGGTAGCC	Pr032067199
jerboa	AGTGAGAGCTCTGCTTTTCGTTTC	GGCAGTAGAAGGCCTGGTAGCC	Pr032067192
horse	CCAGCGAAAACTCTGCTTTT	GATCAATATGGTCAAAACATTTGC	Pr032067185
camel	CCAGCGAAAACTCTGCTTTT	GATCAATATGGTCAAAACATTTGC	Pr032067180
Fgf8			
mouse	TGCTGTGCCTGCAGGCNCARGARGG	CAGCTTGCCCTTCTTGTTCATRCADAT	Pr032067200
jerboa	TGCTGTGCCTGCAGGCNCARGARGG	CAGCTTGCCCTTCTTGTTCATRCADAT	Pr032067193
horse	CCTAATTTTACACAGCATGTGAGG	GGCGGGTAGTTGAGGAACTC	Pr032067186
camel	CCTAATTTTACACAGCATGTGAGG	GGCGGGTAGTTGAGGAACTC	Pr032067181
pig	CAGGGTGTTTCCCAACAGGT	GGCAATCAGCTTCCCCTTCT	Pr032067206

Primer sequences used for amplification and accession numbers for probe sequences are provided for each species and gene.